molecular pharmaceutics

Article

pubs.acs.org/molecularpharmaceutics

Characterization of in Vivo Disulfide-Reduction Mediated Drug Release in Mouse Kidneys

Jun J. Yang,[†,‡,§] Sumith A. Kularatne,[†,‡,∥] Xianming Chen,[⊥] Philip S. Low,*[,†] and Exing Wang*[,⊥,#]

[†]Department of Chemistry, Purdue University, 560 Oval Drive, West Lafayette, Indiana 47907, United States

[⊥]Department of Medicine/Division of Nephrology, Indiana University School of Medicine, R2-268, 950 West Walnut Street, Indianapolis, Indiana 46202, United States

Supporting Information

ABSTRACT: Due to the overexpression of a folate receptor (FR) on many malignant cells, folate-targeted drugs have been developed to improve the cancer specificity of chemotherapeutic agents. Therapeutic index is further enhanced with the use of self-immolative linkers that efficiently release the attached drug upon cellular internalization of the folate−drug conjugate. Because FR is also abundant in normal kidney proximal tubule (PT) cells, we sought to examine in real time the trafficking and release of folate-targeted drugs in the kidney in vivo. Thus, we conducted two-photon kidney imaging studies in mice utilizing a Förster resonance energy transfer (FRET) based folate conjugate that undergoes a color shift from red to green upon reduction of the disulfide bond linking folate to a surrogate drug molecule. Following infusion via intravenous injection, folate−FRET reached the kidney in its intact unreduced form. The folate−FRET conjugate was then filtered into the lumen of PT, where it was efficiently captured by FR. As FR transcytosed across PT, some disulfide reduction occurred, with reduced folate−FRET detectable in PT vesicles 30 min postinjection. Prolonged monitoring of folate−FRET in mice showed modest progression of reduction in PT cells over time. Moreover, inhibition of FR trafficking in PT cells by colchicine did not significantly affect the rate or extent of folate−FRET reduction. Finally, the lack of cytosolic accumulation of released drug surrogate in the PT suggests that drug release via disulfide bond reduction should cause little kidney toxicity.

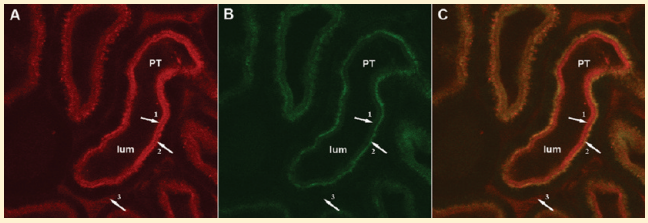

KEYWORDS: *disulfide reduction, drug release, kidney toxicity, FRET (Förster resonance energy transfer), intravital microscopy, two-photon*

INTRODUCTION

In an effort to reduce toxicity to normal tissues, antineoplastic agents are often tethered to high affinity ligands that selectively accumulate in tumors. In particular, folic acid constitutes one of the most frequently employed targeting ligands, largely because its receptor (i.e., folate receptor [FR]) is overexpressed in a wide variety of tumors (e.g., breast, lung, kidney, ovary, colon, brain, and hematologic malignancies)[1−3] yet absent in most normal tissues.[3,4] Folate can be easily conjugated to low- or high-molecular weight therapeutic or imaging agents, and these conjugates bind FR with affinity comparable to folic acid ($K_d \sim 10^{-9}$ M).[5,6] More importantly, FR undergoes internalization via endocytosis, delivering folate (or its therapeutic conjugates) into the cell interior.[7,8] To promote intracellular drug delivery, folate−drug conjugates have been frequently constructed with cleavable linkers (e.g., disulfide linker) that ensure release of the attached drug only after internalization by the target cell.[9−12]

In addition to its overexpression on malignant cells, FR is present on the apical membrane of the proximal tubules (PT) of the kidney, where the receptor is thought to capture folate from the nascent urine filtered through the glomeruli and return it to the blood for use by the organism. As reviewed by Birn,[13] multiple pathways may exist for trafficking the internalized folate complex, as a number of receptors and carrier proteins for folates have been observed in the PT. Using in vivo two-photon microscopy, a folate−Texas Red conjugate was found to accumulate in lysosome-like compartments which were believed to transcytose across the PT cells.[14] However, despite this capture of folate−drug conjugates by PT cells, renal toxicities are extremely rare in preclinical and clinical studies of folate-targeted drugs.[9−11] With the increasing popularity of folate-mediated drug targeting, it is relevant to define the kinetics, location, and determinants of folate−drug conjugate trafficking and processing during transport in the kidney.

Traditional pharmacokinetic techniques often employ radioactive tracers to map the biodistribution of molecules of interest.[15−20] Alternatively, drugs and their metabolites can be extracted from tissues and then identified using sophisticated analytical methods such as LC/MS.[21−25] These two methods, however, are inadequate to study the release of a drug from its targeting ligand, since (1) radiolabeling does not distinguish

Received: September 21, 2011
Revised: December 13, 2011
Accepted: December 15, 2011
Published: December 15, 2011

released drug from its intact precursor, (2) postmortem release of drug from the conjugate is difficult to prevent, and (3) extensive manipulations like extraction are potential causes of artificial drug release. Therefore, a technique that allows real time, noninvasive examination of the release of a targeted drug is needed. To this end, we have developed a Förster resonance energy transfer (FRET)-based imaging method that produces a shift in fluorescence emission from red to green upon release of free drug from folate (the targeting ligand),[26] and therefore allows real-time monitoring of the integrity of the folate−drug conjugate in vivo by two-photon fluorescence microscopy. Using this method, we herein characterize redox-induced drug release during FR-mediated drug conjugate trafficking in the kidney of athymic nude *nu/nu* mice.

METHODS AND MATERIALS

Chemicals. Sulforhodamine methanethiosulfonate (SRMS) was obtained from Toronto Research Chemicals, Inc. (North York, Ontario, Canada), and 4,4-difluoro-4-bora-3a,4a-diaza-*s*-indacene-3-propionic acid, succinimidyl ester (BODIPY FL, SE) was purchased from Invitrogen (Carlsbad, CA). Fluorenylmethyloxycarbonyl (Fmoc)-Cys(trityl)-resin and amino acids were purchased from Novabiochem (San Diego, CA). Benzotriazol-1-yl-oxytripyrrolidinophosphonium hexafluorophosphate (PyBOP) was from Peptide Int. (Louisville, KY). Hoechst 33342 was obtained from Invitrogen (Carlsbad, CA). All other chemicals were purchased from major suppliers. Folate conjugates (folate−FRET, folate−BODIPY, and folate−rhodamine) were synthesized as previously described with minor modifications[26,27] (Supplemental Figure 1 in the Supporting Information).

Animals Preparation. All animal studies were conducted in compliance with the Institutional Animal Care and Use Committee (IACUC) guidelines. Male *nu/nu* mice were purchased from Charles River Laboratories (Wilmington, MA), maintained on a folate deficient diet, and housed in a sterile environment on a standard 12 h light−dark cycle.

Two-Photon Intravital Microscopy. The kidney surgical procedure was performed as described before,[14] except for the use of a height adjustable custom-built mouse kidney cup device needed for the upright microscope in this study. Following anesthetization with intraperitoneal (ip) ketamine (18−20 mg/kg) and xylazine (10−13 mg/kg) injection, the right kidney was exposed surgically by a lateral incision and secured in a kidney cup. The body of the animal was kept warm with a heat pad (Mastex, Petersburg, VA) during surgery. The animal was then transferred with the kidney cup device to the stage of the two-photon microscope for imaging, and the body temperature was maintained at around 37 °C by a home-built temperature control device for the duration of the entire experiments. Depending upon the experimental design, prior to or during imaging, the animals were administered with one of three folate conjugates (1 μmol/kg, in 0.9% NaCl solution), namely, folate−BODIPY, folate−rhodamine, or folate−FRET, via a tail vein catheter and imaged using a two-photon microscope. Some animals were also treated with the nuclear stain Hoechst 33342 (200 μg) via ip injection 30 min prior to imaging.

All images were acquired using a Zeiss LSM 510 two-photon imaging system with an Axioplan2 upright microscope and a 40X C-Apochromat water immersion, NA 1.2. The excitation source was a Spectra-Physics (Mountainview, CA) Ti:Sapphire mode-lock tunable femtosecond pulsed laser. The wavelength was tuned to 930 nm (for optimal BODIPY excitation) or 800 nm (to excite rhodamine and Hoechst dye). To optimize the FRET signal, the excitation wavelength was set to 930 nm because this wavelength is the two-photon peak excitation cross section for the BODIPY dye, and is near the excitation valley for rhodamine.[28] Internal photomultiplier tubes (descanned mode) were used with maximized pinholes. The emission filters of 435−485, 500−550, and 565−615 nm were used for Hoechst, BODIPY, and rhodamine, respectively. The image acquisition speed was approximate 1 frame/s.

Image Processing and Data Analysis. Images were processed using Metamorph (Universal Imaging, West Chester, PA) in combination with a vesicle segmentation program developed at the Indiana Center for Biological Microscopy. Fluorescence quantification was conducted using the method described previously.[29] The saturated pixels were excluded from analysis.

RESULTS

In order to mimic a ligand−drug conjugate where the therapeutic warhead is tethered to folate via a releasable disulfide linker, we have previously designed a folate−FRET construct[26] that is composed of (i) a targeting ligand, namely, folic acid, labeled with a green fluorescent agent, BODIPY, that serves as the FRET donor, and (ii) a red fluorescent agent, rhodamine (the FRET acceptor) that is linked to folate via a reducible disulfide bond (Figure 1). When the two

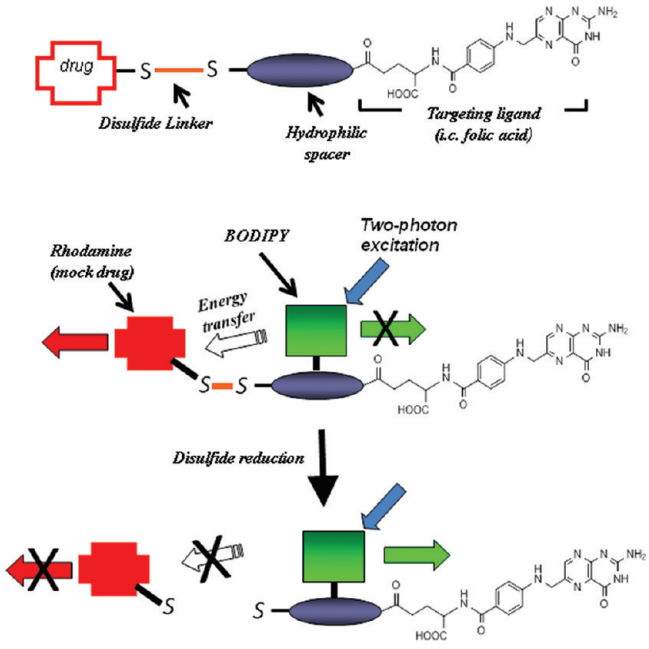

Figure 1. Disruption of intramolecular energy transfer in the folate−FRET reporter after disulfide reduction.

fluorophores are attached to the same folate, excitation of the BODIPY leads to efficient intramolecular Förster resonance energy transfer (FRET), resulting in emission of red fluorescence. Upon disulfide bond reduction, however, rhodamine is released from the folate−FRET conjugate, permitting the attached BODIPY to emit its green fluorescence. Therefore, drug release (separation of fluorophores) can be monitored by measuring the consequent recovery of donor fluorescence

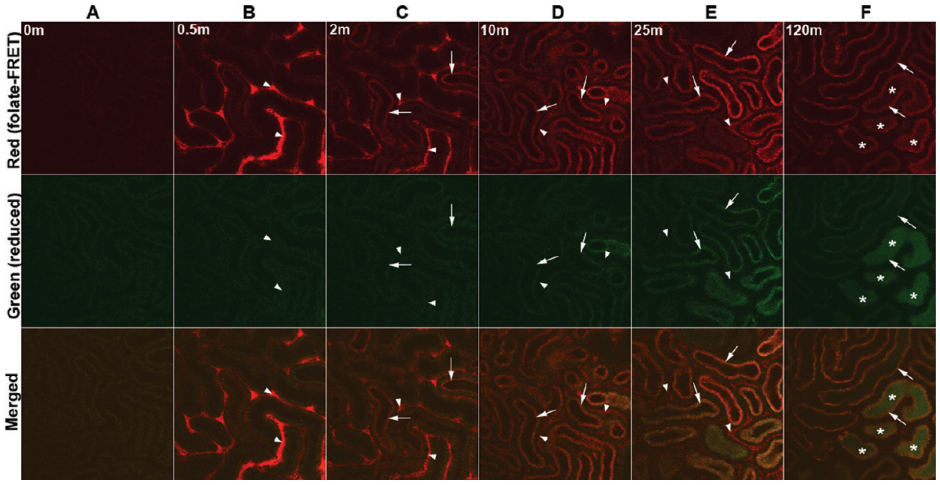

Figure 2. Folate−FRET uptake in the kidney proximal tubule (PT) during 0 to 2 h. The intravital two-photon images were taken following a bolus infusion of folate−FRET reporter (1 μmol/kg) using a Zeiss LSM 510 multiphoton imaging system with an Axioplan2 upright microscope at 930 nm excitation. Before the infusion a very low level of autofluorescence was seen in the PT (A). Strong FRET induced red fluorescence and minimal BODIPY fluorescence from the intact folate−FRET appeared in the plasma (arrow heads) 0.5 min after the infusion (B). At 2 min the filtered folate−FRET (red) quickly bound to the PT apical domain (arrows) (C). At 10 min some reduced folate−BODIPY appeared in the PT, as evidenced by the increased green fluorescence (D, middle panel). At 25 min substantial green fluorescence was seen as more reduced folate−BODIPY appeared in the PT (arrows), while the color of the plasma (arrowhead) remained red (E). At 2 h the overall fluorescence in the PT decreased, but strong green fluorescence was seen in the lumen of some PT segments (F, middle panel). Late convoluted PTs (marked with *) showed higher concentration of folate−BODIPY (F).

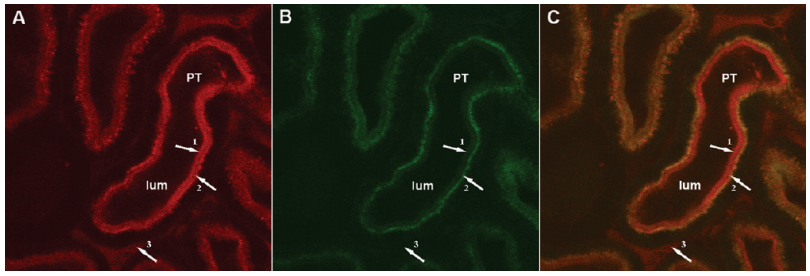

Figure 3. High resolution two-photon in vivo image of the PT after Folate−FRET injection. The image was taken 30 min following the infusion of folate−FRET at 2× zoom for red channel (folate−FRET, panel A), green channel (reduced, panel B), and merged (C). The predominant color in the brush border region (arrow 1) and the plasma (arrow 3) was red, but substantial green fluorescence was present at the subapical region (arrow 2).

(green) and concurrent diminution of acceptor fluorescence (red).

Intravital Kidney Imaging with Folate−BODIPY and Folate−Rhodamine. To determine optimal settings for FRET imaging in vivo, we first examined mice treated with folate−BODIPY (FRET donor alone) or folate−rhodamine (FRET receptor alone). At 930 nm, the proximal tubule (PT) of mice injected with folate−BODIPY showed extremely low signal in the red channel (Supplemental Figure 2A in the Supporting Information), whereas strong fluorescence was observed in the green channel (Supplemental Figure 2B in the Supporting Information), confirming efficient excitation of the BODIPY fluorophore with minimal spectral crosstalk from the green to the red channel. In contrast, mice treated with folate−rhodamine exhibited minimal red fluorescence when excited at 930 nm (Supplemental Figure 2C in the Supporting Information) compared with images taken at 800 nm excitation (Supplemental Figure 2D in the Supporting Information). Taken together, these data demonstrate that 930 nm constitutes a useful wavelength for folate−FRET imaging, because the dynamic range of the FRET signal is maximized by selective excitation of the donor molecule (BODIPY) with minimal direct excitation of the acceptor (rhodamine) and little spectral cross talk.

Intravital Kidney Imaging with Folate−FRET. To monitor in vivo drug release in the kidney, folate−FRET was injected into the tail vein of athymic nude mice and a series of images were taken of the exposed kidney using two-photon microscopy at 930 nm excitation. As seen in Figure 2A, preinjection images of the kidney showed minimal autofluorescence. Immediately following iv bolus infusion of folate−FRET (1 μmol/kg), red fluorescence rapidly appeared in blood vessels (data not shown). The intensity of this red fluorescence reached its peak ~30 s after infusion, while the green signal remained largely indistinguishable from the background (arrow heads, Figure 2B), indicating that the disulfide bond linking the acceptor rhodamine remained intact over this time period in the circulation. Within minutes, the fluorescence signal in the blood significantly subsided (Figure 2C−E, arrow heads) as a result of glomerular filtration, with concurrent increase of FRET fluorescence at the apical domain of the PTs (Figure 2D−F, indicated by arrows), suggesting the filtered folate−FRET molecules now were bound to FR lining the lumen side of PT. While the predominant color of the apical domain of the

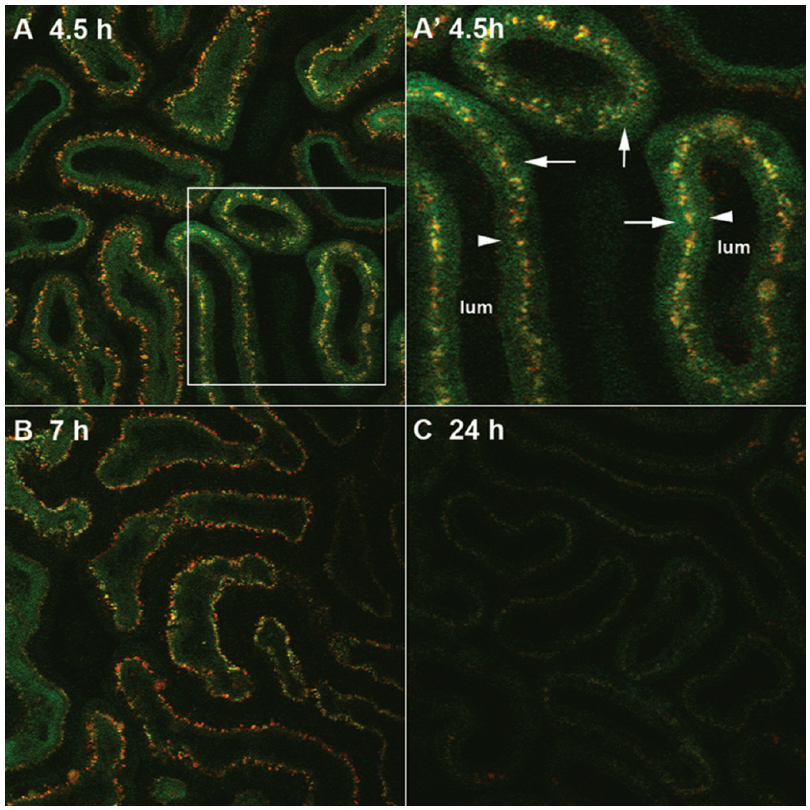

Figure 4. Folate−FRET metabolism in the kidney proximal tubule (PT) over prolonged times. Strong green fluorescence from the reduced folate−BODIPY was seen in the brush border region 4.5 h after folate−FRET treatment. Substantial green fluorescence was also present in the cytosolic region of some PT. The brown color of vesicles demonstrates the colocalization of red and green (A). The highlighted region in A is enlarged and is presented in A′, which clearly shows cytosolic accumulation of the reduced BODIPY−folate (arrows). The brush border is indicated by arrow heads (A′). At 7 h the overall green fluorescence was reduced without substantial changes in the fluorescence distribution pattern (B). At 24 h the secretion and reduction of the folate conjugates was near completion as the overall fluorescence level approached the baseline level.

PT remained red, a gradual increase of green color in the same region was observed, indicating gradual accumulation of reduced folate−FRET conjugate (Figure 2D,E). Twenty-five minutes postinfusion, increased green fluorescence was observed at the apical domain of the PT point (Figure 2E), although the blood vascular structures were still visible only in the red channel.

A higher resolution image (zoom 2×) taken 30 min after the infusion reveals fluorescence pattern at a subtubular level (Figure 3). The brush border region (arrow 1) of the PT was now dominated by red color (Figure 3A), whereas the subapical region (arrow 2), presumably containing the endosomal compartments, showed substantial green signal (Figure 3B, and appeared orange in the merged image, Figure 3C). Because most of the folate−FRET agent at this 30 min time point was still intact in the bloodstream (arrow 3), the subapical green fluorescence must have resulted from disulfide reduction within the PT cells.

Images taken 2 h after infusion of folate−FRET (Figure 2F) show an apparent decrease of the overall fluorescence in the PT cells probably due to secretion and redistribution processes. Meanwhile, however, strong fluorescence, predominantly green, also appeared in some segments of the PT lumen (Figure 2F, indicated by asterisk), suggesting that any residual folate conjugates remaining in circulation at this long time point had been reduced to folate−BODIPY. These segments morphologically resembled the late, not early, convoluted PT, where more of the filtered water had been reabsorbed and the filtrate was concentrated.[30,31]

At 4.5 h, the red brush border of PT seen at earlier time points now became predominantly green (Figure 4A), plausibly as a consequence of FR-mediated capture of reduced folate−FRET (i.e., folate−BODIPY). Unlike the uniform color observed in the brush border, the subapical regions contained compartments with distinct fluorescence: green, orange, and red colors. We postulate that such the heterogeneity of these vesicles reflected differential degree of folate−FRET reduction and/or was a result of subsequent endocytic sorting.[26] In addition, diffuse fluorescence staining was visible in some (albeit not all) PT cells at this time point (Figures 4A and 4A′), consistent with cytosolic accumulation of the reduced complex. At 7 h, the red/green fluorescence distribution pattern remained largely unchanged from 4.5 h, although overall signal intensity of the PT cells was reduced substantially (Figure 4B). By 24 h (Figure 4C), the disappearance of the remaining folate complexes from the PT was almost complete, as evidenced by the extremely low overall fluorescence intensity in the PT. Although little fluorescence remained at this time point, the dominant color within the PT cells, including majority of the lysosomal compartments, became green, indicating near completion of disulfide bond reduction of any folate conjugate that was retained.

Intravital Kidney Imaging with Folate−FRET after Colchicine Treatment. To further determine the role of vesicle trafficking in folate−FRET reduction, we performed

dx.doi.org/10.1021/mp200483t | *Mol. Pharmaceutics* 2012, 9, 310−317

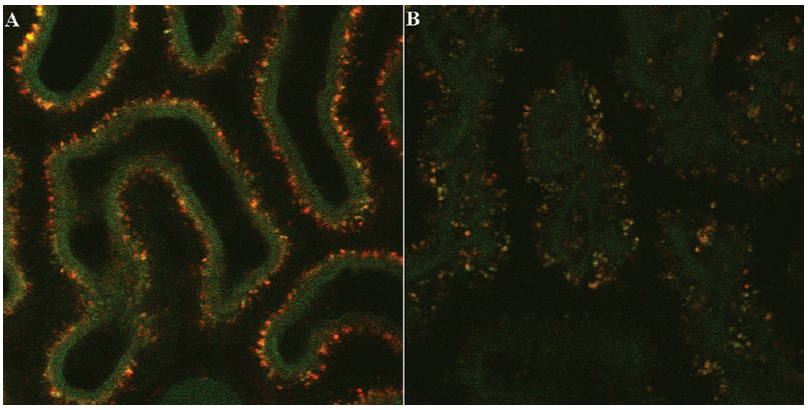

Figure 5. Effect of colchicine treatment on kidney uptake of the folate–FRET. Images were taken from mice with (B) or without (A) colchicine treatment for 7 h, but both were treated with folate–FRET for the last 4 h prior to imaging. An overall decrease in fluorescence intensity was seen in the treated mouse.

intravital kidney imaging in colchicine-treated mice (3.2 mg/kg body wt administrated ip). As demonstrated previously,[14] uptake of the folate conjugate in the PT was severely hindered in mice pretreated with this inhibitor of microtubule polymerization. Thus, kidney images taken 7 h after colchicine administration and 4 h following folate–FRET treatment revealed a substantially lower overall uptake of folate–FRET compared to control animals (Figure 5). Interestingly, the degree of folate–FRET disulfide bond reduction in the PT was minimally affected by colchicine. Quantitative fluorescence ratio analysis confirmed that the green/red (folate–BODIPY/folate–FRET) ratio within the segmented vesicles in the PT cells was similar under both conditions (0.53 ± 0.065 for the untreated and 0.50 ± 0.17 for colchicine-treated) (Figure 6).

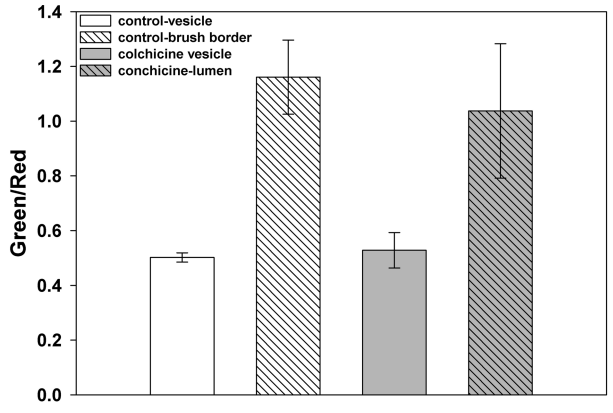

Figure 6. Quantitation of green/red (i.e., reduced/intact folate–FRET) fluorescence ratios. The fluorescence ratio in the vesicles was obtained after segmentation as described in the Methods and Materials. The green/red (reduced/intact folate–FRET) ratio within the segmented vesicles in the proximal tubule (PT) cells was 0.53 ± 0.065 for the untreated and 0.50 ± 0.17 for the colchicine-treated mice. A much higher ratio was found in the brush border region for both treated (1.04 ± 0.24) and untreated mice (1.16 ± 0.14). However, the difference between the treated and untreated in both ratios (either at the brush border or within the subapical vesicles) was not significant.

The brush border region of PT exhibited a higher green/red ratio than subapical vesicles in both treated (1.04 ± 0.24) and untreated mice (1.16 ± 0.24), probably due to FR recapture of reduced folate–FRET (folate–BODIPY) at this time point as described above (Figure 4A). The dark PT lumen and the bright brush border, which were clearly visible in the untreated mouse (Figure 5A), were indistinguishable in the treated mouse (Figure 5B). Supplemental Figures 3A–C in the Supporting Information show an example of a folate–FRET image (red, green, and merged) and the same image after vesicle segmentation (Supplemental Figure 3D in the Supporting Information) which was used for the quantitative fluorescence ratio analysis. The similar green/red ratios in the untreated and treated mice from both vesicles and the brush border suggest that the level of nonrenal disulfide bond reduction was much higher than that in the PT cells.

■ DISCUSSION

The objective of this study was to develop an in vivo two-photon FRET imaging method to investigate the efficiency of disulfide bond reduction and consequent drug release from folate-targeted disulfide-bridged prodrugs in the kidney. To this end, a folate–FRET conjugate that changes fluorescence from red to green upon reductive cleavage of an intramolecular disulfide bond was used as a model system. Analysis of the data suggests that folate receptor-targeted disulfide-linked drugs (i) remain intact in blood circulation for at least 30 min, (ii) rapidly localize to FR on the apical membrane of the PTs, (iii) undergo partial but incomplete reduction during endocytic trafficking in PTs, (iv) are reduced during prolonged circulation outside of the kidney, and (v) eventually clear from the kidneys.

Our data indicate that drug release occurring in the kidney is modest. Green fluorescence (indicative of drug release) at the subapical region of PT cells increased rapidly during the first 30 min after infusion of folate–FRET (Figures 2 and 3), followed by a rather slow disulfide bond reduction over a long period of time, even after the brush border had become predominately green (Figure 4). If the same initial rapid rate of disulfide reduction within the PTs had been sustained, a higher green/red ratio in the vesicles at later time points would have been observed. Additionally, the fact that colchicine treatment did not have any measurable effect on the rate of disulfide reduction, both in the interior and exterior of PT cells, supports the contention that only a small fraction of the disulfide reduction occurred within kidney PT cells.

Because some reduction of the intramolecular disulfide bond linking folate to its surrogate drug (rhodamine) was seen in these studies, the question naturally arises why kidney toxicity is

not seen when similarly structured folate-targeted cytotoxic agents are administered to either animals or humans (unpublished data). Although an unequivocal answer cannot be provided from our data, we wish to offer three possible explanations. First, although quantitative measurement of the fraction of folate conjugate that was reduced to free drug by the kidneys was not possible, analysis of the ratio of free rhodamine to intact folate−FRET arriving at the kidneys from the bloodstream could be assessed from the ratio of these two components in the brush border compartment. As noted in the control mice (not exposed to colchicine) in Figure 5A, most of the disulfide reduction had already occurred by 4 h after folate−FRET treatment, as evidenced by the green color in the brush border region of the PT as opposed to the brown color seen in the endosomal compartments. Thus, most release of free drug would have occurred elsewhere in the body by this time point. Moreover, since folate conjugates are cleared from the blood with a half time of only 5 min in mice and 20 min in humans,[32,33] the fraction of folate conjugates available for cleavage in the blood at this 4 h time point may be too small to impact patient toxicity. Second, no evidence of free rhodamine (drug surrogate) could be detected in the cytosol (data not shown). Although a slow accumulation of reduced folate−BODIPY fragment was seen in the cytosol of some PT cells at longer time points (Figures 4A and 4A′), it would not have any impact on the cytosolic level of free drug. More discussion on this is given below. Finally, because PT cells are bordered on one side by blood vessels and on the other side by urine space, any released drug might be washed or diluted away before it could damage the PT. In any case, it does not appear that sufficient quantities of cytotoxic drugs remain in the PT to damage kidney function.

With a glomerular sieving coefficient of 0.7,[34] folates are rapidly filtered by the kidneys. In fact, it has been calculated that humans would become folate deficient within 15 min in the absence of an efficient salvage pathway for the vitamin. FRs are primarily expressed on the apical brush-border membrane of kidney PT cells,[35−39] and FR-mediated capture and transport of the vitamin back into the bloodstream has been found to be saturable.[34,40,41] But, the question still remains as to how the kidney can maintain an efficient salvage system with a limited capacity against such a rapid clearance pathway. Interestingly, intense staining persisted in the brush border region (Figures 3−5) even hours after folate−FRET administration and when the overall fluorescence in cytoplasm had become low. This observation supports proposed mechanism that suggests folates might be sequestered and retained by PT cells.[14] It is also possible that some internalized folate constructs could be returned to the apical surface multiple times before eventually being moved to the basolateral surface for release into the blood.

PT uptake of folate is characterized by a rapid luminal entry and a subsequent slow cytoplasmic transport.[41] The precise mechanism of folate uptake and trafficking by the kidneys, however, has not been fully elucidated. Our data and previous studies[14] indicate that despite rapid uptake, internalized folate is not stored in large quantities within the PT cell cytoplasm. Mechanisms by which internalized folate is released to the bloodstream are of great interest. Sandoval et al. employed two-photon microscopy to track a folate−Texas Red conjugate during its trafficking through the PTs in live mice.[14] These authors found that the majority of folate conjugate internalized by PTs accumulated within a lysosomal compartment initially. The folate containing compartment, however, was subsequently sorted away from lysosomal compartment and slowly moved from the apical to the basolateral domain of the cell via a transcytotic pathway. Meanwhile, in these studies no cytosolic accumulation of the folate conjugate was detected within an hour following folate−Texas Red treatment. Interestingly, our result shows that 4.5 h after bolus infusion of folate−FRET, a significant amount of disulfide reduced folate−BODIPY fragment can be seen in cytosolic regions of some PT cells (Figure 4A). One possibility is that the cytosolic accumulation of reduced folate−BODIPY fragment was a result of a nonspecific uptake.[42] With a much less efficient rate compared to a receptor mediated uptake, the non-carrier-mediated transport would presumably have little impact on renal toxicity, as the drug release, mediated by a reducible disulfide bond, would have occurred elsewhere long before drug concentration in the cytosol could reach a toxic level. In fact, our data show that even though the released rhodamine accumulated within vesicular compartments in the PT cells, rhodamine was never detected in the cytosolic region. However, we cannot exclude the possibility that the cytosolic accumulation of the reduced folate−BODIPY construct was a result of a slow release from the vesicular compartment after separation from the receptor. Together with evidence which suggests that substantial disulfide reduction occurred outside the kidneys, we conclude that a significant portion of the internalized folate−FRET in PT cells underwent FR-mediated transtubular transport from the lumen back to the bloodstream largely intact. To accomplish this, an effective transcytotic mechanism, as demonstrated previously,[14] is likely involved.

■ ASSOCIATED CONTENT

Supporting Information

Figures depicting chemical structures of folate−FRET, folate−rhodamine, and folate−BODIPY conjugates; folate−BODIPY and folate−rhodamine conjugate uptake in the kidney tubules; and endosome segmentation of kidney proximal tubule of a mouse treated with folate−FRET for quantitative fluorescence ratio analysis. This material is available free of charge via the Internet at http://pubs.acs.org.

■ AUTHOR INFORMATION

Corresponding Author

*E.W.: Department of Cellular and Structural Biology, University of Texas Health Science Center at San Antonio, STRF, RM-252, San Antonio, TX 78229; phone, 210-562-4062; e-mail, wange3@uthscsa.edu. P.S.L.: Department of Chemistry, Purdue University, 560 Oval Drive, West Lafayette, IN 47907; phone, 765-494-5273; fax, 765-494-5272; e-mail, plow@purdue.edu.

Present Addresses

[§]Department of Pharmaceutical Sciences, St. Jude Children's Research Hospital, Memphis, TN 38105.

[∥]Department of Chemistry, The Scripps Research Institute, 10550 North Torrey Pines Road, La Jolla, CA 92037.

[#]Department of Cellular and Structural Biology, University of Texas Health Science Center at San Antonio, San Antonio, TX 78229.

Author Contributions

[‡]J.J.Y. and S.A.K. contributed equally to this study.

■ ACKNOWLEDGMENTS

This work was supported by Purdue University/Indiana University School of Medicine collaboration in biomedical research pilot grant (P.S.L. and E.W.) and P30 DK079312 Center for Advanced Renal Microscopic Analysis pilot grant (E.W.). The authors wish to thank Drs. I.R. Vlahov, C.P. Leanion, and H.K. Santhapuram for their valuable insight, and Dr. G.A. Tanner for his critiques and comments on the manuscript.

■ REFERENCES

(1) Bueno, R.; Appasani, K.; Mercer, H.; Lester, S.; Sugarbaker, D. The alpha folate receptor is highly activated in malignant pleural mesothelioma. *J. Thorac. Cardiovasc. Surg.* **2001**, *121* (2), 225−33.

(2) Parker, N.; Turk, M. J.; Westrick, E.; Lewis, J. D.; Low, P. S.; Leamon, C. P. Folate receptor expression in carcinomas and normal tissues determined by a quantitative radioligand binding assay. *Anal. Biochem.* **2005**, *338* (2), 284−93.

(3) Ross, J. F.; Chaudhuri, P. K.; Ratnam, M. Differential regulation of folate receptor isoforms in normal and malignant tissues in vivo and in established cell lines. Physiologic and clinical implications. *Cancer* **1994**, *73* (9), 2432−43.

(4) Weitman, S. D.; Lark, R. H.; Coney, L. R.; Fort, D. W.; Frasca, V.; Zurawski, V. R. Jr.; Kamen, B. A. Distribution of the folate receptor GP38 in normal and malignant cell lines and tissues. *Cancer Res.* **1992**, *52* (12), 3396−401.

(5) Low, P. S.; Henne, W. A.; Doorneweerd, D. D. Discovery and development of folic-acid-based receptor targeting for imaging and therapy of cancer and inflammatory diseases. *Acc. Chem. Res.* **2008**, *41* (1), 120−9.

(6) Low, P. S.; Kularatne, S. A. Folate-targeted therapeutic and imaging agents for cancer. *Curr. Opin. Chem. Biol.* **2009**, *13* (3), 256−62.

(7) Anderson, R. G.; Kamen, B. A.; Rothberg, K. G.; Lacey, S. W. Potocytosis: sequestration and transport of small molecules by caveolae. *Science* **1992**, *255* (5043), 410−1.

(8) Kamen, B. A.; Smith, A. K. A review of folate receptor alpha cycling and 5-methyltetrahydrofolate accumulation with an emphasis on cell models in vitro. *Adv. Drug Delivery Rev.* **2004**, *56* (8), 1085−97.

(9) Leamon, C. P.; Reddy, J. A.; Vlahov, I. R.; Westrick, E.; Parker, N.; Nicoson, J. S.; Vetzel, M. Comparative preclinical activity of the folate-targeted Vinca alkaloid conjugates EC140 and EC145. *Int. J. Cancer* **2007**, *121* (7), 1585−92.

(10) Leamon, C. P.; Reddy, J. A.; Vlahov, I. R.; Westrick, E.; Dawson, A.; Dorton, R.; Vetzel, M.; Santhapuram, H. K.; Wang, Y. Preclinical antitumor activity of a novel folate-targeted dual drug conjugate. *Mol. Pharmaceutics* **2007**, *4* (5), 659−67.

(11) Leamon, C. P.; Reddy, J. A.; Vetzel, M.; Dorton, R.; Westrick, E.; Parker, N.; Wang, Y.; Vlahov, I. Folate targeting enables durable and specific antitumor responses from a therapeutically null tubulysin B analogue. *Cancer Res.* **2008**, *68* (23), 9839−44.

(12) Henne, W. A.; Doorneweerd, D. D.; Hilgenbrink, A. R.; Kularatne, S. A.; Low, P. S. Synthesis and activity of a folate peptide camptothecin prodrug. *Bioorg. Med. Chem. Lett.* **2006**, *16* (20), 5350−5.

(13) Birn, H. The kidney in vitamin B12 and folate homeostasis: characterization of receptors for tubular uptake of vitamins and carrier proteins. *Am. J. Physiol.* **2006**, *291* (1), F22−36.

(14) Sandoval, R. M.; Kennedy, M. D.; Low, P. S.; Molitoris, B. A. Uptake and trafficking of fluorescent conjugates of folic acid in intact kidney determined using intravital two-photon microscopy. *Am. J. Physiol.* **2004**, *287* (2), C517−26.

(15) Kularatne, S. A.; Wang, K.; Santhapuram, H. K.; Low, P. S. Prostate-specific membrane antigen targeted imaging and therapy of prostate cancer using a PSMA inhibitor as a homing ligand. *Mol. Pharmaceutics* **2009**, *6* (3), 780−9.

(16) Dunphy, M. P.; Lewis, J. S. Radiopharmaceuticals in preclinical and clinical development for monitoring of therapy with PET. *J. Nucl. Med.* **2009**, *50* (Suppl. 1), 106S−21S.

(17) Schibli, R.; Schubiger, P. A. Current use and future potential of organometallic radiopharmaceuticals. *Eur. J. Nucl. Med. Mol. Imaging* **2002**, *29* (11), 1529−42.

(18) Siegel, B. A.; Dehdashti, F.; Mutch, D. G.; Podoloff, D. A.; Wendt, R.; Sutton, G. P.; Burt, R. W.; Ellis, P. R.; Mathias, C. J.; Green, M. A.; Gershenson, D. M. Evaluation of 111In-DTPA-folate as a receptor-targeted diagnostic agent for ovarian cancer: initial clinical results. *J. Nucl. Med.* **2003**, *44* (5), 700−7.

(19) Leamon, C. P.; Parker, M. A.; Vlahov, I. R.; Xu, L. C.; Reddy, J. A.; Vetzel, M.; Douglas, N. Synthesis and biological evaluation of EC20: a new folate-derived, (99m)Tc-based radiopharmaceutical. *Bioconjugate Chem.* **2002**, *13* (6), 1200−10.

(20) Wang, S.; Luo, J.; Lantrip, D. A.; Waters, D. J.; Mathias, C. J.; Green, M. A.; Fuchs, P. L.; Low, P. S. Design and synthesis of [111In]DTPA-folate for use as a tumor-targeted radiopharmaceutical. *Bioconjugate Chem.* **1997**, *8* (5), 673−9.

(21) Tolonen, A.; Turpeinen, M.; Pelkonen, O. Liquid chromatography-mass spectrometry in in vitro drug metabolite screening. *Drug Discovery Today* **2009**, *14* (3−4), 120−33.

(22) Chen, C.; Gonzalez, F. J.; Idle, J. R. LC-MS-based metabolomics in drug metabolism. *Drug Metab. Rev.* **2007**, *39* (2−3), 581−97.

(23) Maurer, H. H. Current role of liquid chromatography-mass spectrometry in clinical and forensic toxicology. *Anal. Bioanal. Chem.* **2007**, *388* (7), 1315−25.

(24) Xu, R. N.; Fan, L.; Rieser, M. J.; El-Shourbagy, T. A. Recent advances in high-throughput quantitative bioanalysis by LC-MS/MS. *J. Pharm. Biomed. Anal.* **2007**, *44* (2), 342−55.

(25) Wiseman, J. M.; Ifa, D. R.; Zhu, Y.; Kissinger, C. B.; Manicke, N. E.; Kissinger, P. T.; Cooks, R. G. Desorption electrospray ionization mass spectrometry: Imaging drugs and metabolites in tissues. *Proc. Natl. Acad. Sci. U.S.A.* **2008**, *105* (47), 18120−5.

(26) Yang, J.; Chen, H.; Vlahov, I. R.; Cheng, J. X.; Low, P. S. Evaluation of disulfide reduction during receptor-mediated endocytosis by using FRET imaging. *Proc. Natl. Acad. Sci. U.S.A.* **2006**, *103* (37), 13872−7.

(27) Vlashi, E.; Sturgis, J. E.; Thomas, M.; Low, P. S. Real time, noninvasive imaging and quantitation of the accumulation of ligand-targeted drugs into receptor-expressing solid tumors. *Mol. Pharmaceutics* **2009**, *6* (6), 1868−75.

(28) Xu, C.; Webb, W. W. Measurement of two-photon excitation cross sections of molecular fluorophores with data from 690 to 1050 nm. *J. Opt. Soc. Am. B* **1996**, *13* (3), 481−91.

(29) Wang, E.; Brown, P. S.; Aroeti, B.; Chapin, S. J.; Mostov, K. E.; Dunn, K. W. Apical and basolateral endocytic pathways of MDCK cells meet in acidic common endosomes distinct from a nearly-neutral apical recycling endosome. *Traffic* **2000**, *1* (6), 480−93.

(30) Giebisch, G.; Windhager, E. E. Renal tubular transfer of sodium, chloride and potassium. *Am. J. Med.* **1964**, *36* (5), 643−669.

(31) Liu, F. Y.; Cogan, M. G. Axial heterogeneity in the rat proximal convoluted tubule. I. Bicarbonate, chloride, and water transport. *Am. J. Physiol.* **1984**, *247* (5), F816−821.

(32) Leamon, C. P.; Parker, M. A.; Vlahov, I. R.; Xu, L.-C.; Reddy, J. A.; Vetzel, M.; Douglas, N. Synthesis and Biological Evaluation of EC20: A New Folate-Derived, 99mTc-Based Radiopharmaceutical. *Bioconjugate Chem.* **2002**, *13* (6), 1200−1210.

(33) Li, J.; Sausville, E. A.; Klein, P. J.; Morgenstern, D.; Leamon, C. P.; Messmann, R. A.; LoRusso, P. Clinical pharmacokinetics and exposure-toxicity relationship of a folate-Vinca alkaloid conjugate EC145 in cancer patients. *J. Clin. Pharmacol.* **2009**, *49* (12), 1467−76.

(34) Goresky, C. A.; Watanabe, H.; Johns, D. G. The Renal Excretion of Folic Acid. *J. Clin. Invest.* **1963**, *42* (12), 1841−9.

(35) Birn, H.; Selhub, J.; Christensen, E. I. Internalization and intracellular transport of folate-binding protein in rat kidney proximal tubule. *Am. J. Physiol.* **1993**, *264* (2 Part 1), C302−10.

(36) Corrocher, R.; Abramson, R. G.; King, V. F.; Schreiber, C.; Dikman, S.; Waxman, S. Differential binding of folates by rat renal

cortex brush border and basolateral membrane preparations. *Proc. Soc. Exp. Biol. Med.* **1985**, *178* (1), 73−84.
(37) Hjelle, J. T.; Christensen, E. I.; Carone, F. A.; Selhub, J. Cell fractionation and electron microscope studies of kidney folate-binding protein. *Am. J. Physiol.* **1991**, *260* (2 Part 1), C338−46.
(38) Holm, J.; Hansen, S. I.; Hoier-Madsen, M.; Bostad, L. A high-affinity folate binding protein in proximal tubule cells of human kidney. *Kidney Int.* **1992**, *41* (1), 50−5.
(39) Selhub, J.; Franklin, W. A. The folate-binding protein of rat kidney. Purification, properties, and cellular distribution. *J. Biol. Chem.* **1984**, *259* (10), 6601−6.
(40) Birn, H.; Nielsen, S.; Christensen, E. I. Internalization and apical-to-basolateral transport of folate in rat kidney proximal tubule. *Am. J. Physiol.* **1997**, *272* (1 Part 2), F70−8.
(41) Selhub, J.; Emmanouel, D.; Stavropoulos, T.; Arnold, R. Renal folate absorption and the kidney folate binding protein. I. Urinary clearance studies. *Am. J. Physiol.* **1987**, *252* (4 Part 2), F750−6.
(42) Muldoon, R. T.; Ross, D. M.; McMartin, K. E. Folate Transport Pathways Regulate Urinary Excretion of 5-Methyltetrahydrofolate in Isolated Perfused Rat Kidney. *J. Nutr.* **1996**, *126* (1), 242−50.